Article:
Lei, H. orcid.org/0009-0005-9922-2520, Zhang, Y. orcid.org/0000-0002-9736-5043 and Khandelwal, B. orcid.org/0000-0001-9295-188X (2025) Numerical investigation of geometric design effect on micromix hydrogen combustion. Fuel, 401. 135657. ISSN: 0016-2361

https://doi.org/10.1016/j.fuel.2025.135657

Title: Numerical Investigation of Geometric Design Effect on Micromix Hydrogen Combustion

Author: Huanrong Lei[a] (雷桓荣), Yang Zhang[a], Bhupendra Khandelwal[b],

Affiliations:

[a] Mechanical Engineering, Faculty of Engineering, University of Sheffield, Sheffield S10 2TN, UK

[b] Mechanical Engineering Department, University of Alabama, Tuscaloosa, Alabama

Corresponding Author:

Huanrong Lei, [a] hleistargazer@gmail.com, [b] yz100@sheffield.ac.uk

Address:

Department of Mechanical Engineering

Sir Frederick Mappin Building

Mappin Street

Sheffield

S1 3JD

Abstract

This paper addressed to the optimisation of the hydrogen micromix combustor design. Building on the existing micromix concept, the micromix combustor geometry was modified to enhance the NO_X reduction capability. The internal geometric parameters, such as mixing distance and air gate height, were optimised and numerically studied. The results convincingly demonstrated a significant influence of geometric modifications on combustion performance. NO_X emissions produced during combustion were successfully reduced by changing the internal geometry of the micromix combustor, and a clear relationship between NO_X emission variation and geometric parameter changes was concluded. The results showed that increasing the mixing distance improves the air/fuel mixing, contributing to lower NO_X production, while a lower air gate design reduces the temperature along the chamber and resulted in the NO_X reduction.

Keywords

Micromix combustion; Fuel-air mixing; Hydrogen; NO_X emission; CFD Modelling

1. Introduction

The rapid growth of the aviation industry has made air travel indispensable; however, the increased use of traditional fossil fuels raises significant environmental concerns. Currently, Kerosene and AVGAS are the primary aviation fuels, emitting substantial greenhouse gases, contributing to climate change. Carbon dioxide emissions from the combustion of traditional fossil fuels continue to increase over time[1]. These fuels also pose economic challenges as non-renewable resources with increasing prices. To address these challenges, there is a growing interest in alternative clean energy sources. The report "WAYPOINT 2050" from Air Transport Action Group stated in the next three decades after 2050, sustainable fuels will be the way to reduce or even zero carbon emissions in the aviation industry [2]. Hydrogen power emerges as a promising solution for clean applications in the aviation industry. Unlike conventional fossil fuels, hydrogen combustion produces only water and nitrogen oxides as by-products,

offering numerous advantages. Hydrogen fuel is not only a clean energy source but also boasts the highest energy density, with approximately 120 MJ/kg (excluding the radioactive element)[3].

However, utilizing hydrogen fuel in conventional combustors poses challenges due to its distinct physical properties, including a high burning speed, large diffusivity, and a wide flammability range. In addition, the high combustion temperature of hydrogen increases NO_X emissions [4], [5], [6]. Overcoming issues like auto-ignition risk and high NO_X emissions is essential for the safe and efficient use of hydrogen fuel in existing combustors [7].

The challenge of hydrogen combustion technology is an important part of development of hydrogen fuelled gas turbine power. At the present, the most extensively used hydrogen combustion concept is refining large-scale flames into numerous micro flames, which can significantly increase the mixing rate, thereby improve the mixing uniformity[8], [9], [10]. This new mixing strategy is defined as “micromix”, the conventional swirling mixing channel is replaced by multiple micro mixing channels which are generally smaller than 10mm in size. In each micro mixing channel, the enhanced mixing technology is adopted such as Jet-in-Cross-Flow, swirling mixing, axial jet in mixing flow etc. The individual mixing channel significantly improves the mixing intensity of air and fuel and generate a cluster of micro flames, which help fuel mix with air sufficiently and reduce the residence time during combustion.

The concept of micromix combustion was first developed in the 1990s by the research team at Aachen University of Applied Sciences (AcUAS) for hydrogen combustion. By multiplying the mixing zones, the design significantly enhanced hydrogen-air mixing intensity and uniformity, effectively reducing NO_X emissions. As noted by Dahl and Suttrop [11], the concept aims to "minimise the scale of mixing and maximise the mixing intensity." Over the past 30 years, AcUAS has advanced hydrogen micromix diffusion combustion technology through six generations [12].

Through these generations, the JICF injection and diffusive combustion was used and each hydrogen injector was paired with an air gate. This technology was applied to a GTCP36-300 annular combustor with 1600 injection element [13], [14]. Their researches focused on optimization of the JICF injection and bluff body placement improved the understanding of vortex structures and combustion behavior

[15]; identifying key parameters such as blockage ratio, injector diameter, injection depth, and recirculation zones [13], [16], [17], [18], [19], [20]. Subsequently, AcUAS further optimised the dual-fuel operation capability [20], [21], [22], [23], [24], [25], and developed the a 2MW dry-low- NO_X industry rich-hydrogen gas turbine and only produced 35ppm NO_X during the cooperation with Kawasaki Heavy Industries company (KHI) since 2011 [25], [26], [27].

Theoretically, the micromix combustion concept employs a rapid mixing strategy based on Jet-in-Crossflow (JICF) injection to address the insufficient mixing intensity typical of diffusive combustion. Hydrogen and air are injected through crossflow nozzles, forming a high-velocity jet that enters the combustion chamber. Due to the extremely small nozzle diameter, the resulting jet velocity exceeds the flame propagation speed of hydrogen, effectively mitigating the risk of flashback. At the same time, the high-velocity jet forms a stable shear layer that serves as a flame anchoring zone. Downstream, stable inner and outer recirculation vortices are generated by the bluff body and air guiding panel (Figure 1), reducing the residence time of the combustion products in high-temperature zones, thus lowering NO_X emissions. Moreover, a multi-nozzle array configuration is adopted to replace the conventional combustor design (Figure 2), improving the uniformity of temperature distribution. The flame clusters formed by millimeter-scale nozzles establish stable micro-flame structures, significantly reducing the issue of localized high temperatures during hydrogen combustion [28], [29].

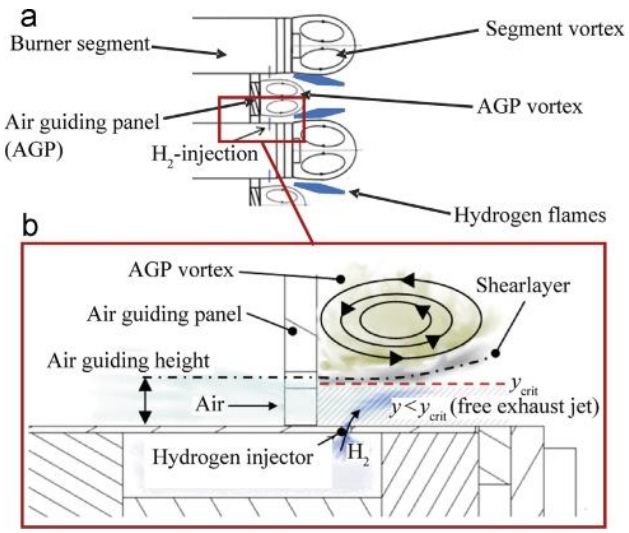

Figure 1.(a) Aerodynamic flame stabilization principle, (b) hydrogen injection depth definition [13].

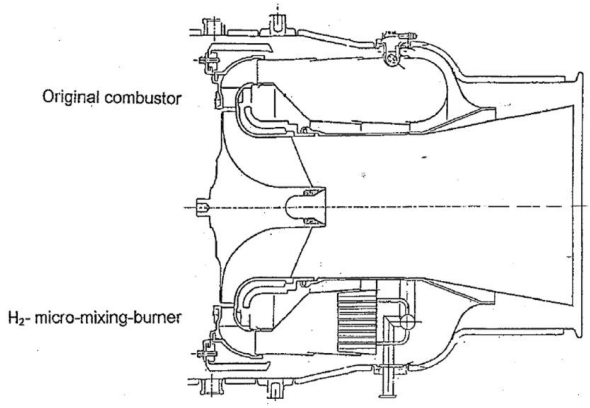

Figure 2. Structural layout of the APU GTCP 36-300 combustion chamber and turbine in original configuration (top) and equipped with a Micromix Module (bottom) [11].

The micromix diffusion combustion technology has been widely recognized as one of the safest and most effective solutions for preventing flashback and achieving stable hydrogen combustion. Many subsequent designs of hydrogen combustor have adopted some of the concepts of micromix combustion. From the previous studies, it could be found that the micromix combustion performance is very sensitive to the mixing characteristics which is dominated by the flow behaviour in the chamber. The effect of geometric parameters to combustion performance and NO_X emission was continuously investigated by many different researchers.

For the typical micromix combustor, Cranfield University has carried out a lot of research based on the 5th generation micromix combustor since 2018. With the support of ENABLE H2 project, they systematically obtained the influence of multiple key parameters on the combustor performance and emissions such as the air gate shape and injection method. Additionally, the thermoacoustic instability problem of micromix combustor has also been studied [30], [31], [32], [33], [34]. Lopez et al. conducted a series of studies about the variable APG panel dimensions and flexible fuel, they successfully maintained the main characteristics of the micromix combustion with different burner geometry and ED value[35], [36], [37]. J. Berger studied two different designs and focused on the effect air gate aspect ratio and hydrogen injection diameter to the NO_X emissions[38].

Mo et al. conducted a numerical study on the flow dynamic and combustion performance of the hydrogen honeycomb micromix combustor with triangular bluff bodies in the air gate, they studied the effect between flow structure and bluff body It shown that the NO_X emission is sensitive to the

dimension of bluff body[39], [40]. Devriese et al. analyse the mechanism of JICF in micromix combustion, they studied on the impact of injection pressure and air mass flow rate on the injection depth and defined the best range of these factors to control the wall temperature[41], [42].

The concept of micromix was adopted by different pure hydrogen/rich-hydrogen combustor designs. Harbin Institute of Technology (HIT) team started the research about micromix combustion recent years, they design a hydrogen rich micromix burner which use JICF on a mixing tube, the premixing method was used in their design [43], [44]. They conducted the numerical investigation of fuel/air mixing characteristics of single nozzle and stated that the fuel hole shape and the diameter of the air tube have great influence on the vortex and vorticity. Zhao et al from HIT did research about the characteristics of swirl/non-swirl micromix flames, they found that the NO_X emission was lower with the swirling flow and the mixing intensity was affect by momentum ratio greatly[45].

There were many different hydrogen combustor designs using the multiple injection elements design. In these studies, the burner geometry was simplified, the multiple mix tube with JICF mechanism were applied. Liu et al. from CAS designed a multi-nozzle array model combustor, the multi-injection method is similar to the micromix concept, the mixing point is at the front end of the mixing tube, it is more like a partial premix combustion[46], [47]. This design shown that the stage combustion could improve the thermoacoustic instability problem. Durocher et al. researched the combustion characterization of a 5-nozzle array micromix injection burner, and improve the stability and combustion dynamics[48].

In summary, micromix combustion as one of the best hydrogen combustion solution, is still being studied in depth by various teams around the world. There are still many scientific concepts worth exploring in micromix combustion. In particular, the dynamic changes in the flow field caused by structural optimisation have an impact on the mixing characteristics and flame structure, which greatly affects the temperature performance of the combustion chamber and NO_X emissions.

This study focuses on optimising the internal geometry of micromix hydrogen combustor, particularly by modifying mixing distance on step bluff body and air gate design. The geometric parameters are investigated for their influence on NO_X emissions. Previous works demonstrated that optimising the physical structure of a micromix burner can significantly enhance combustion performance and reduce NO_X formation. Their findings highlight the critical role of flow dynamics in emission characteristics.

Accordingly, this study emphasizes the impact of flow dynamics on combustion performance. Suitable numerical models are evaluated and applied to simulate micromix hydrogen combustion. By analyse the relationship between flow dynamic and mixing characterises in the combustor with various geometry parameters, study the performance of micromix combustion. The research focus of this paper is to summarize the impact of changes in the internal geometric structure of the combustion chamber on combustion performance and NO_X emissions, and to form a multi-physics field coupling mechanism of flow field and combustion to support future micromix combustion investigations.

2. Configuration and Numerical method

2.1 Combustor Geometry

In the micromix combustor, hydrogen fuel is injected perpendicular to the air stream through the air gate. This jet-in-crossflow (JICF) method effectively enhances the fuel/air mixing intensity. By adjusting the burner geometry, the mixing and combustion performance can be further optimized. The basic configuration of the micromix combustor is illustrated below. Figure 3 (a) displays the prototype hydrogen micromix combustor from FHA, featuring 1600 miniaturized injection elements. In most laboratory studies, a simplified micromix burner is utilized, as demonstrated in Figure 3 (b). Due to the numerous numbers of injectors, the angle between the burner elements can be negligible in the lab-scale study.

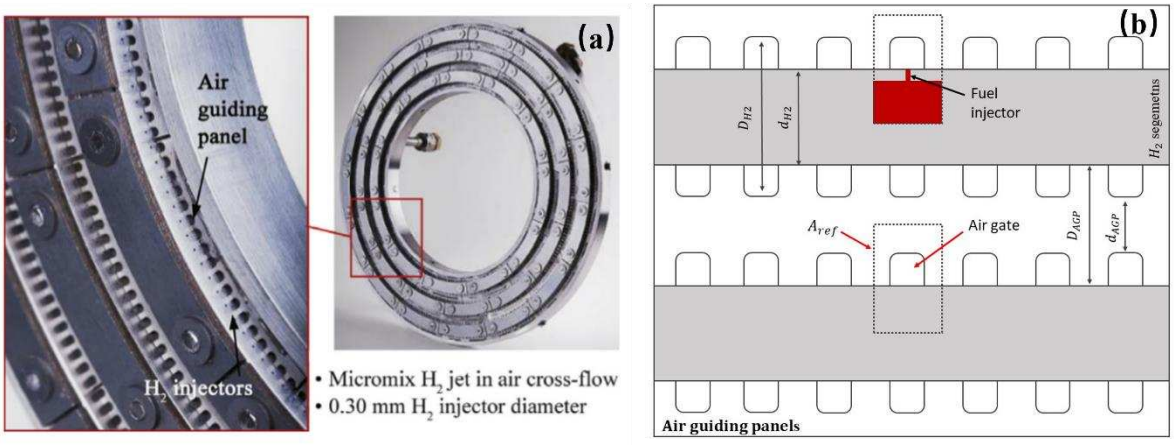

Figure 3.(a) Micromix prototype combustor for APU CTCP 36-300. (b) Schematic drawing of simplified micromix combustor.

In this study, to investigate the geometrical parameters, only a single injection element is analysed to save the computational resources and time. The geometric model of a single burner is depicted in Figure 4 below, referring to the region within the dashed-line box in Figure 3 (b). The geometry shown below is the flow domain in the combustor; it is a sectional slice of the flow domain of the entire test burner. Considering one injection element, its size is extremely small, and the corresponding combustion zone is confined within a domain of approximately 3 mm * 10 mm. In the experimental burner, the diameter of the hydrogen injection pipe is 0.3 mm. To validate the numerical methods, the dimensions used for the single injection element are based on the studies by Ayed and his teams [49], [50], [51]. Because the single injection element is symmetric in both X and Y directions, four sides in the X and Y directions are defined as symmetry planes. Apart from these four symmetry planes, the inlets and outlet, the other boundaries are defined as walls. The wall sections in Figure 4 are highlighted in green colour, the symmetrical boundaries are highlighted in yellow.

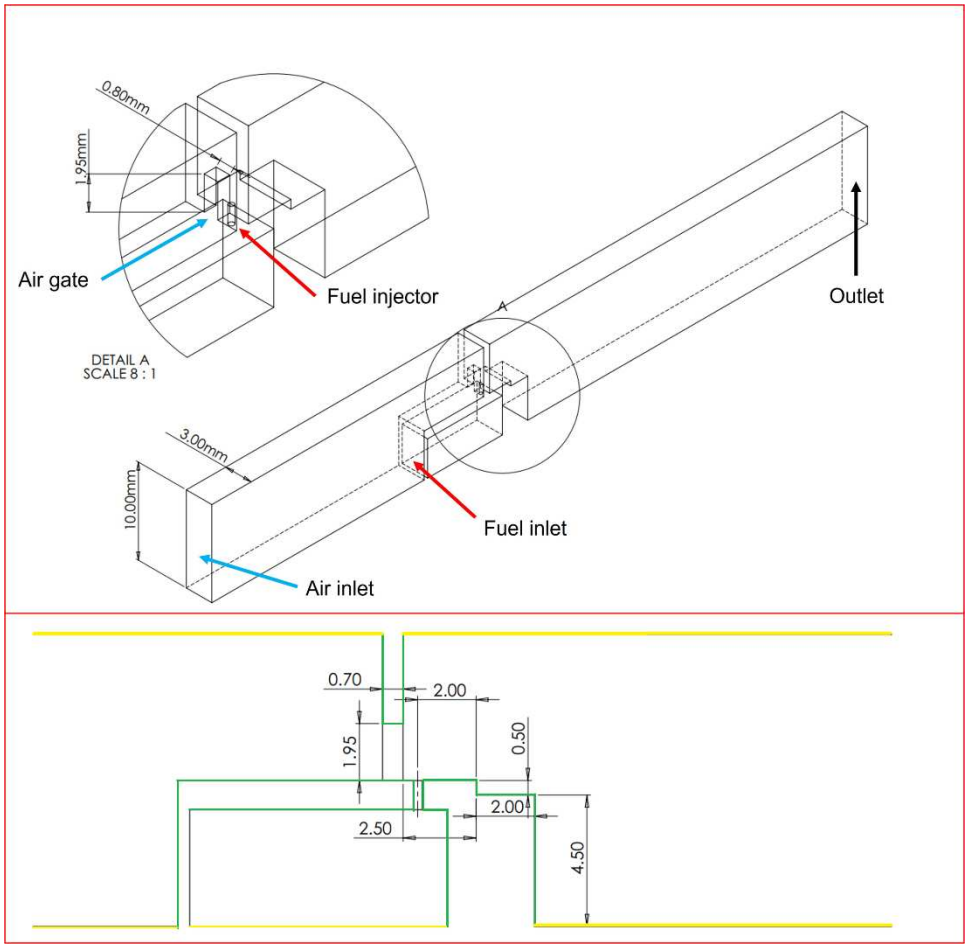

Figure 4. Geometry showing of single hydrogen micromix combustor.

The jet-in-crossflow design used in micromix combustor could enhance the mixing of air and fuel. As the figure illustrated, with the design of the air guiding panel (AGP), the air stream flow through the air gate and accelerated, then the hydrogen fuel injected into the air stream and form the inner vortex structure in the burner. For hydrogen combustion due to the high combustion temperature, the injection depth y is an important factor. The paper states that the low injection depth could cause the high temperature at the near wall area and cause material, but the over-deep injection could cause the penetration and increase the NO_X formation, it is important to find an optimal momentum ratio and injection depth for different design [52]. In this micromix concept combustion, the injection depth should be controlled less than the critical depth y_{crit} to prevent the hydrogen flow penetrate the shear layer into the inner vortex, in that case the combustion will occurs in the vortex area and cause the high NO_X formation.

$$r = \frac{\rho_{H2} V^2{}_{H2}}{\rho_{air} V^2{}_{air}} \tag{1}$$

$$y \sim \alpha \cdot d_{H2} \cdot \sqrt{r} \tag{2}$$

Where V is the velocity of gases mixing, which is the air velocity through the air gate and hydrogen velocity being injected in. r is the momentum flux ratio, it decides the injection depth y. From the paper [53], the value of α could be defined as 2, hence the preliminary calculation of each case could be calculated. The momentum flux ratio is dependent on the air/fuel velocities and their density. By optimising the air gate, these values could be controlled to reach the satisfied combustion performance.

2.2Boundary Conditions

The normalised energy density (ED_n) of this single injection element is 6.7 MW/m^{2}bar, representing the thermal power design demand and referring to the energy of the designed combustor zone.

$$ED_n = \frac{E_{ref}}{A_{ref} \times P_{ref}} \left[\frac{MW}{m^2 bar}\right] \tag{3}$$

Where E_{ref} is the reference thermal energy of a single injection element, A_{ref} is the cross-sectional area of single injector combustion which is labelled in the Figure 3 (b) shown above. For the boundary conditions used for the basic burner design, the inlet temperature of air and fuel are 550K and 300K respectively, the operation pressure is 1 bar. The simulation results will be compared to the reference

experimental data from Ayed et al. studies[54] for validation purpose. In the following studies, the normalised energy density will remain the same, the inlet velocity of air would vary with different equivalence ratio conditions.

2.3Numerical method

The numerical studies in this paper were performed by using computational fluid dynamics (CFD) with the software ANSYS FLUENT 2021 R2 in double precision. To obtain simulation results that closely match experimental data, it is essential to select appropriate turbulence and combustion model.

2.3.1 Turbulence model

For the researchers, they need to make trade-offs between accuracy and computational cost. Reynolds-averaged Navier-Stokes (RANS) models were considered by many researchers because of their low computational cost and good prediction accuracy [55]. For these micromix combustion studies, RANS model could provide accurate results, this model has been validated by other research in their works [56], [57], [58], [59], [60]. The numerical solutions were validated with experimental data and proved the capability of RANS models in micromix combustion study.

In this study, the shear-stress transport (SST) $\mathrm{k}-\omega$ model by Menter [61], [62] was selected Compared to $\mathrm{k}-\varepsilon$ model and standard $\mathrm{k}-\omega$ model, the SST $\mathrm{k}-\omega$ model considers the transport of the shear stress in turbulence and refines the model constants. Furthermore, this model effectively combines the advantages of near-wall region prediction of the $\mathrm{k}-\omega$ model and the free-stream independence of the $\mathrm{k}-\varepsilon$ in the far field[63]. For the specific micromix combustion simulation, SST $\mathrm{k}-\omega$ model was used by many researchers, they shown the feasibility of this model in micromix burner studies[64], [65]. The transport equations of SST $\mathrm{k}-\omega$ model is shown below [66], compared to the equation of the standard $\mathrm{k}-\omega$ model, the model constants are different, in addition, the term cross-diffusion D_ω was added.

$$\frac{\partial}{\partial t}(\rho k)+\frac{\partial}{\partial x_i}(\rho k u_i)=\frac{\partial}{\partial x_j}\left(\boldsymbol{\Gamma_k}\frac{\partial_k}{\partial x_j}\right)+G_k-Y_k+S_k \tag{4}$$

$$\frac{\partial}{\partial t}(\rho\omega) + \frac{\partial}{\partial x_i}(\rho\omega u_i) = \frac{\partial}{\partial x_j}\left(\boldsymbol{\Gamma_\omega}\frac{\partial_\omega}{\partial x_j}\right) + G_\omega - Y_\omega + D_\omega + S_\omega \quad (5)$$

In this general equation (4) (5) of SST k − ω model, G_k is the production of turbulence kinetic energy k, and G_ω represents the generation of specific dissipation rate ω. Y_k and Y_ω represent the dissipation of k and ω due to the turbulence. The expression equation $\boldsymbol{\Gamma_k}$ and $\boldsymbol{\Gamma_\omega}$ which is the effective diffusivity of k and ω are shown below.

$$\boldsymbol{\Gamma_k} = \mu + \frac{\mu_t}{\sigma_k} \quad (6)$$

$$\boldsymbol{\Gamma_\omega} = \mu + \frac{\mu_t}{\sigma_\omega} \quad (7)$$

The introduction of the cross-diffusion the term D_ω makes the SST k − ω model combines the standard k − ε model and standard k − ω model. The equation shows the detail of D_ω.

$$D_\omega = 2(1 - F_1)\rho\frac{1}{\omega\sigma_{\omega,2}}\frac{\partial_k}{\partial x_j}\frac{\partial_\omega}{\partial x_j} \quad (8)$$

2.3.2 NO_X formation

In the combustion of hydrogen, there are two paths of NO_X produce, thermal NO_X formation and prompt NO_X formation. Prompt NOx is generated in low-temperature, fuel-rich conditions and contributes only to a small portion of the overall NO_X emission during combustion. The major pollutant is thermal NO_X, which is highly dependent on combustion temperature. To predict the formation of NO_X, Fluent employs the extended Zeldovich mechanism, which involves two reactions for NO formation from nitrogen and oxygen at high temperatures, and a third reaction involving the hydroxyl radical [67]. The NO_X formation pathway could be represented by the following equations[68]:

$$O + N_2 \rightleftharpoons N + NO \quad (9)$$

$$N + O_2 \rightleftharpoons O + NO \quad (10)$$

$$N + OH \rightleftharpoons H + NO \quad (11)$$

Based on the reactions above, the formation rate of thermal NO could be represented as the equation (12) below:

$$\frac{d[NO]}{dt} = 2k_{f,1}[O][N_2]\frac{\left(1-\frac{k_{r,1}k_{r,2}[NO]^2}{k_{f,1}[N_2]k_{f,2}[O_2]}\right)}{\left(1+\frac{k_{r,1}[NO]}{k_{f,2}[O_2]+k_{f,3}[OH]}\right)}\left(\frac{mol}{m^3}-s\right) \quad (12)$$

In the equation above, $k_{f,1}$, $k_{f,2}$, $k_{f,3}$ is the forward reaction rate constant, the reverse rate constant is expressed as $k_{r,1}$, $k_{r,2}$ and $k_{r,3}$. These constants are expressed as follow:

$$k_{f,1} = 1.8\times10^{8}e^{-38370/T}, \qquad k_{r,1} = 3.8\times10^{7}e^{-425/T},$$

$$k_{f,2} = 1.8\times10^{4}Te^{-4680/T}, \qquad k_{r,2} = 3.81\times10^{3}e^{-20820/T},$$

$$k_{f,3} = 7.1\times10^{7}e^{-450/T}, \qquad k_{r,3} = 1.7\times10^{8}e^{-24560/T},$$

In this study, thermal NOx is identified as the major pollutant during hydrogen combustion due to its strong dependence on combustion temperature, as mentioned previously. Therefore, to improve the NO_X reduction capability of micromix burner, it is crucial to decrease the combustion temperature. Thus, reducing the combustion temperature by optimising the burner design is the primary objective of this paper. In Fluent, the NO_X emissions are calculated as the mole fraction. To the unify the units, the equations below are used to convert the NO_X from mole fraction to ppm.

$$NOx_{general}\ [ppm] = X_{NOx}[mole]\times10^{6} \quad (13)$$

$NOx_{general}\ [ppm]$ is the value of the NO_X emission directly converted from the calculated value, $X_{NOx}\ [mole]$ is the mole fraction obtained from Fluent. However, considering the oxygen concentration in the experiment is 15%, the values of the NO_X in ppm need to be further corrected with the steps below.

$$NOx_{Correct}\ [ppm] = NOx_{general}\times\frac{21-15}{21-X_{O2}*100} \quad (14)$$

$$NOx_{dry}\ [ppm] = NOx_{Correct}\times\frac{1}{1-X_{H2O}[mole]} \quad (15)$$

In the following studies, the NO_X emission will be presented in the unit [ppm].

2.3.3 Mesh Independence

In this study, a high-quality mesh was generated using the structured mesh method for all subsequent simulations with ICEM software. The meshing strategy involves varying cell density across different

regions. As shown in Figure 5, the crossflow air stream and the combustion reaction zone have increased mesh density to accurately capture the flow intricacies. Conversely, near the outlet, the cell width is larger, reducing the number of mesh elements in this less critical region to save computational costs. Although the SST $k-\omega$ model has advantage at the near wall region, in mesh strategy, the mesh cells at the near wall region are increased to modelling the flow behaviour. The burner size is very small especially the hydrogen pipe size, the cross jet in flow at this region would greatly affect the flow field, so the mesh of pipe wall and the walls at the hydrogen outlet are denser to provide the accurate predictions. Based on experience from other papers [69], [70], [71], the authors conducted the mesh independence studies. For such small-scale of micromix combustor element, the mesh includes approximately 700000 to 1000000 cells would be sufficient for the numerical study purposed.

In this study, the mesh independence study was conducted as well. To determine a reasonable mesh density, the minimal mesh cells number starts from 850000, and increasing the mesh number gradually to ensure the accuracy of calculation. Four mesh independence cases with different cell numbers (850000, 1350000, 1890000, 2300000) were simulated. The results of NO_X formation and temperature along the Z-axis of combustor is shown in Figure 6. The results for different mesh numbers of cases show a very high degree of overlap. It is evident that a mesh number great than one million is sufficient, the mesh density in this range would not affect the accuracy of the numerical result. To balance prediction accuracy and computational efficiency, the number of mesh elements in subsequent simulations will be controlled at approximately 1,500,000 which is in the independence test range.

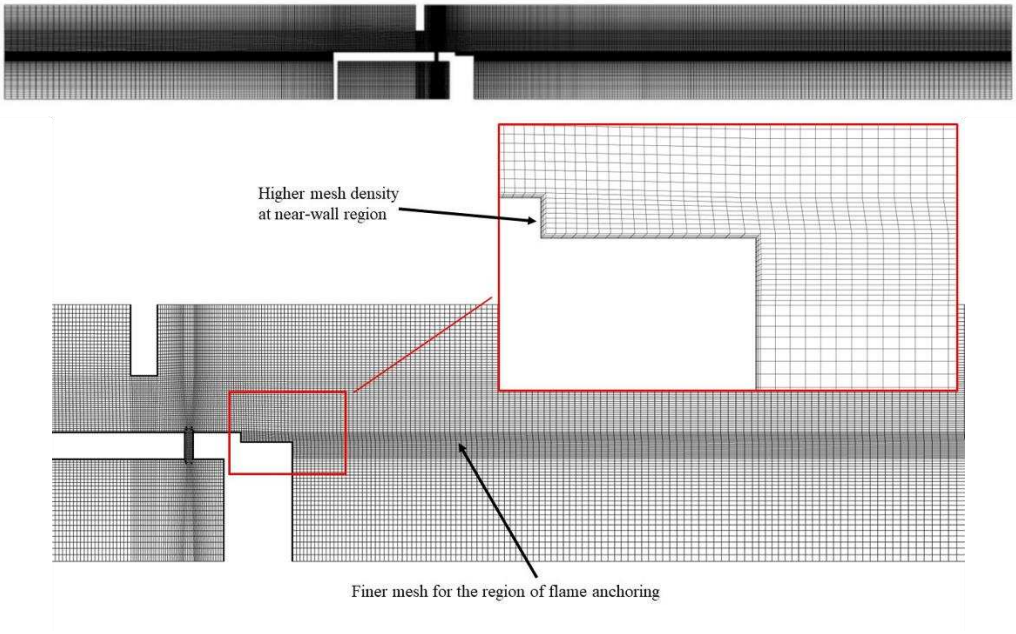

Figure 5. The mesh structure of the basic burner.

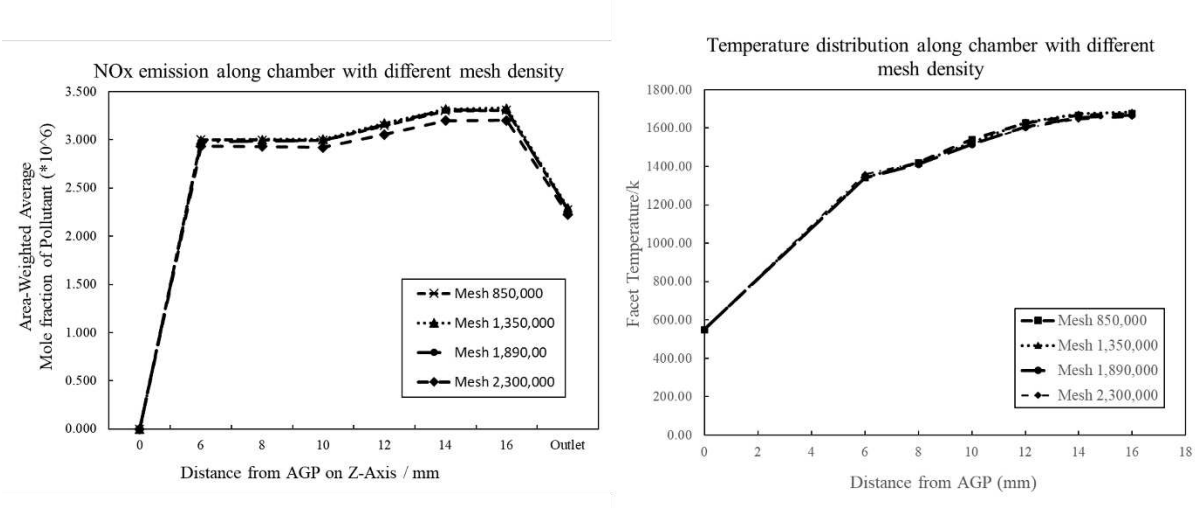

Figure 6. NO_X emission and temperature on the Z-axis of combustor for different mesh numbers.

2.3.4 Combustion model

For this study, due to the high reaction rate of hydrogen, the finite rate eddy dissipation (FR/ED) model and eddy dissipation concept (EDC) model were selected. The FR/ED model combines the eddy dissipation model (EDM) for turbulent mixing-driven reactions and chemical kinetic rate based on the Arrhenius equation. Given this characteristic, the FR/ED could be considered for hydrogen combustion. The EDC model was also selected as it is widely used in numerical studies and is capable of calculating

detailed species reactions during combustion. Additionally, based on the previous numerical studies of micromix combustion [49], both the FR/ED model and EDC model demonstrated good prediction capabilities with micromix combustion.

2.3.5 Mechanism Selection and Validation

Before conducting the simulation study of the combustor geometry, it is crucial to verify the feasibility and accuracy of the numerical methods. For accurate simulation results, selecting appropriate hydrogen reaction mechanisms is essential. In this study, considering factors such as the time of publication, breadth of application, and practical application situations, seven different mechanisms were studied and evaluated, Table 1 below provides details of these mechanisms. Subsequently, Hong 2011 [72] mechanisms, ELTE-2015 mechanism [73] from Eötvös University and Li-2015 from Xiaoyu Li et al. [74] were selected and compared to the experimental data.

Mechanism	**No. of species**	**No. of reactions**	**Ar/He**	**Reference**
Ó Conaire-2003	10	21	x/-	[75]
Zsély-2005	10	32	x/-	[76]
Hong-2011	12	25	x/-	[77]
Creck-2012	11	33	x/x	[78]
Kéromnès-2013	12	33	x/x	[79]
Li-2015	11	25	x/x	[80]
ELTE-2015	12	30	x/x	[81]

Table 1. The summary of the selected hydrogen reaction mechanism.

For validation purposes, the NO_X emission at the exit of the burner was calculated in ppm, the numerical results were compared to the measured data from literature[49]. The NO_X emissions of different mechanisms were calculated at various operational conditions, with the equivalence ratio of mixing increasing from 0.35 to 0.54. A comparison of the calculated NO_X emissions is presented in Figure 7. The results indicate that the NO_X emission at the burner outlet deviates significantly from experimental results when using the Hong-2011 mechanism. However, both the ELTE-2015 and Li-2011 mechanisms performed well in predicting NO_X emissions, with simulation results showing good agreement with the

measured data, especially when using the FR/ED model. As the equivalence ratio increased, the predictions remained accurate. The EDC model predictions, however, showed increasing deviations from the experimental data as the equivalence ratio increased.

For further studies, the ELTE-2015 mechanism was selected because it provided predictions of NO_X emissions that exhibited high agreement with experimental data. Additionally, this mechanism was specially optimised for hydrogen combustion, including the OHEX (excited state) sub-mechanisms.

As a skeletal mechanism, although compare to the large, complete mechanism, the accuracy and the reaction details may not good enough, this mechanism was developed based on the studies of many different hydrogen mechanism, the research results by Olm et al. presented a detailed investigation and shown the capability of this mechanism[82]. For this study, by trade off the accuracy and computational resources, this mechanism was selected for the subsequent works. Overall, it was concluded that further modelling studies of optimised design could be conducted using the selected numerical methods.

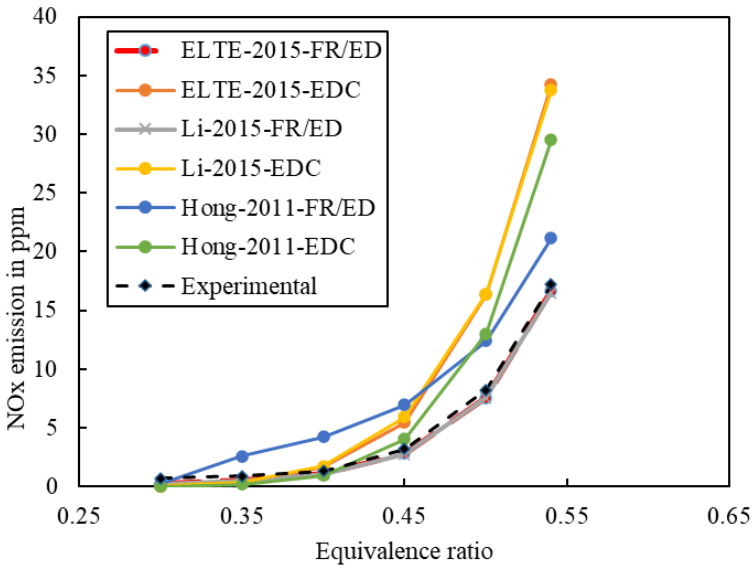

Figure 7.NO_X emission prediction with selected mechanisms.

3. Result and Discussion

3.1Geometric Parameters Optimisation

In this paper, the geometric parameters of a single micromix combustor element were optimised to reduce the NO_X formation during combustion. In the micromix concept, mixing intensity dominates the

317 combustion temperature and NO_X formation level. Therefore, the key design point is to improve air/fuel
318 mixing through physical modifications. To maintain the consistent thermal density, the overall
319 dimensions of the injection element remain the same, while the internal geometry, as shown in Figure
320 8,is modified to investigate the NO_X emission variations. Based on experience and theory [60], [64],
321 [83], the dimensions of the mixing field can effectively influence mixing intensity, thus affecting the
322 amount of NO_X emissions produced.
323 This paper investigates two key parameters: the air/fuel mixing distance (x) and the air gate height (h).
324 The primary research objective is to investigate the effect of these geometric parameter changes on NO_X
325 pollutant emission for the purpose of low NO_X emission hydrogen micromix combustor design.
326 For all the design cases, the energy density is kept at 6.7MW, the fuel inlet amount remains constant,
327 and the air inlet velocity varies based on different equivalence ratios. The combustion model used for
328 this part is mainly the FR/ED model, the EDC model is also applied to calculate the NO_X emission. The
329 main purpose is to study the trend of NO_X variation. Therefore, even if the simulated results of the EDC
330 model do not perfectly match the real measurements, the performance of the optimised cases can still
331 be evaluated by comparing the trend of the emission reduction capability.

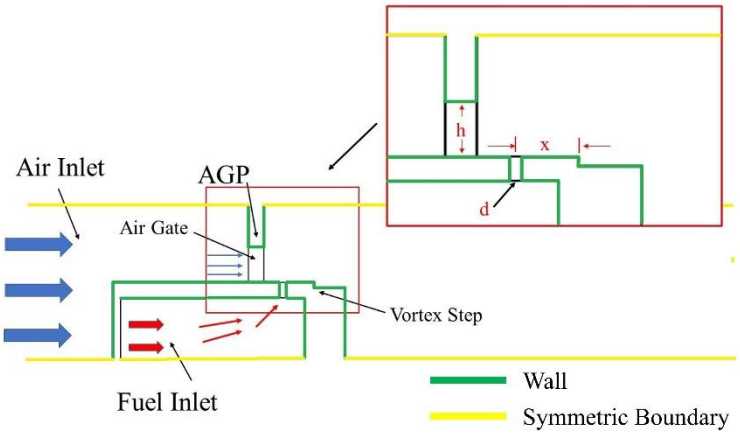

332
333 Figure 8. The annotation of the micromix combustor geometry.

334 3.2Effect of the mixing distance on NO_X emission

335 In this study, the mixing distance (x) of the micromix combustor was modified in four cases: the original
336 basic burner M0 (x: 2mm) and optimised cases M1 (x: 3mm), M2 (x: 4.5mm), and M3 (x: 6mm).

Figure 9 demonstrates the NO_X emissions at the burner outlet for case M0-M3. From the plot, the trend in NO_X emissions change could be intuitively observed: as the mixing distance increases, the NO_X emission drops rapidly, particularly in the range of the length from 3mm to 6mm.

In the results of the FR/ED model simulation group, the NO_X emissions were reduced by about 40%, while the EDC model predicted an even greater reduction of about 50%. Initially, the downward trend was not significant from 2mm to 3mm, the NO_X emissions difference between basic case M0 and M1 was only 0.05ppm with the FR/ED model, indicating that the change of mixing distance is not effective. However, after extending the mixing distance to 4.5mm, NO_X emissions decreased significantly. Both the combustion models showed the NO_X emission trend that the design objective was achieved, the results support the idea that the NO_X emission could be reduced by enlengthening the mixing distance.

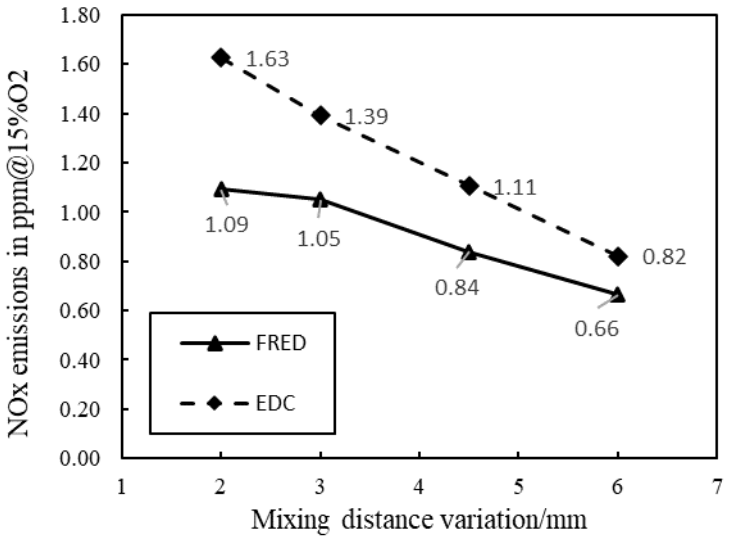

Figure 9.The effects of mixing distance on NO_X emission.

In Figure 10, the flow structures inside the micromix combustor are illustrated. In this typical micromix burner structure, the formation of vortices is significant to the fuel-air mixing and flame stabilization. These designs aim to increase the mixing intensity of the fuel and air, and the velocity pathline shown below confirm that a longer mixing distance effectively increase the vortex size formed in the chamber. The size of the inner vortex increases progressively from cases M0 to M3, with minimal differences observed between M0 and M1. This result aligns with the findings above, indicating that a mixing distance longer than 3mm substantially improves the size growth of the vortex.

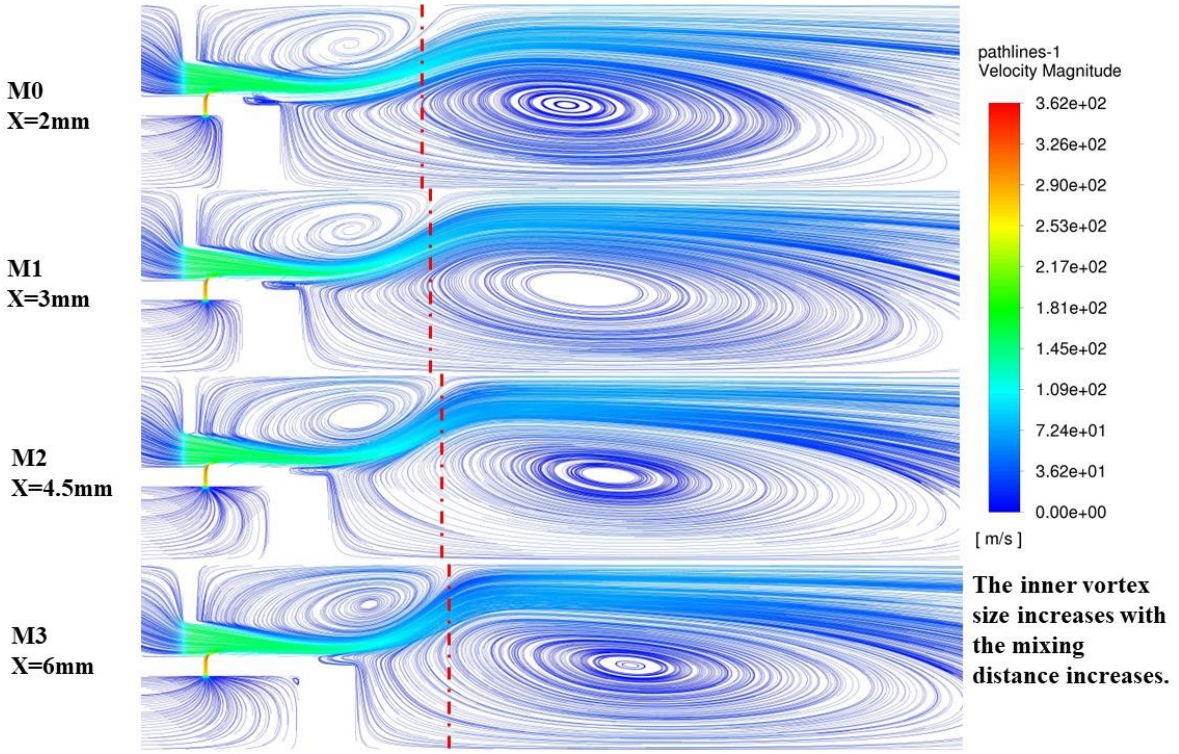

Figure 10. The vortex structure change of the micromix combustor designs

In accordance with the results presented in Figure 11, the NO_X emissions concentration decreased dramatically from case M0 to M3. As the mixing distance increases, the NO_X peak area narrows. The contour plot of NO_X distribution reveals that high NO_X emissions are formed along the shear layer where the flame is anchored. The reduction in the size of the high NO_X field indicates a decrease in the amount of NO_X emissions.

Figure 12 demonstrates that extending the mixing distance significantly improves the mixing intensity of fuel/air. The gray-scale contour of local equivalence ratio inside the chamber illustrates that in case M3, the color at the inner vortex is darker compared to the other cases, the local equivalence ratio increase indicates that more fuel was involved into the air flow and form a highly mixed inner vortex. The rotation of the mixed flow improves the mixing intensity in this region. The vorticity magnitude contour line in Figure 12 furtherly evidence this point, the bigger hollowed area in the vorticity contour indicates the rotational intensity in this area is stronger. Comparing the vorticity contours, with the mixing distance increases the red-lines (high vorticity) become denser. The higher magnitude vorticity along the flow direction drives more fuel and air rotate and increase the mixing. Looking back to Figure 10, the enlargement of the inner vortex also proves this point, the simple extending of the mixing

distance could greatly increase the inner vortex size and the mixing ability. It indicates that the longer mixing distance improve the fuel/air mixing and reduce the incomplete combustion in the chamber.

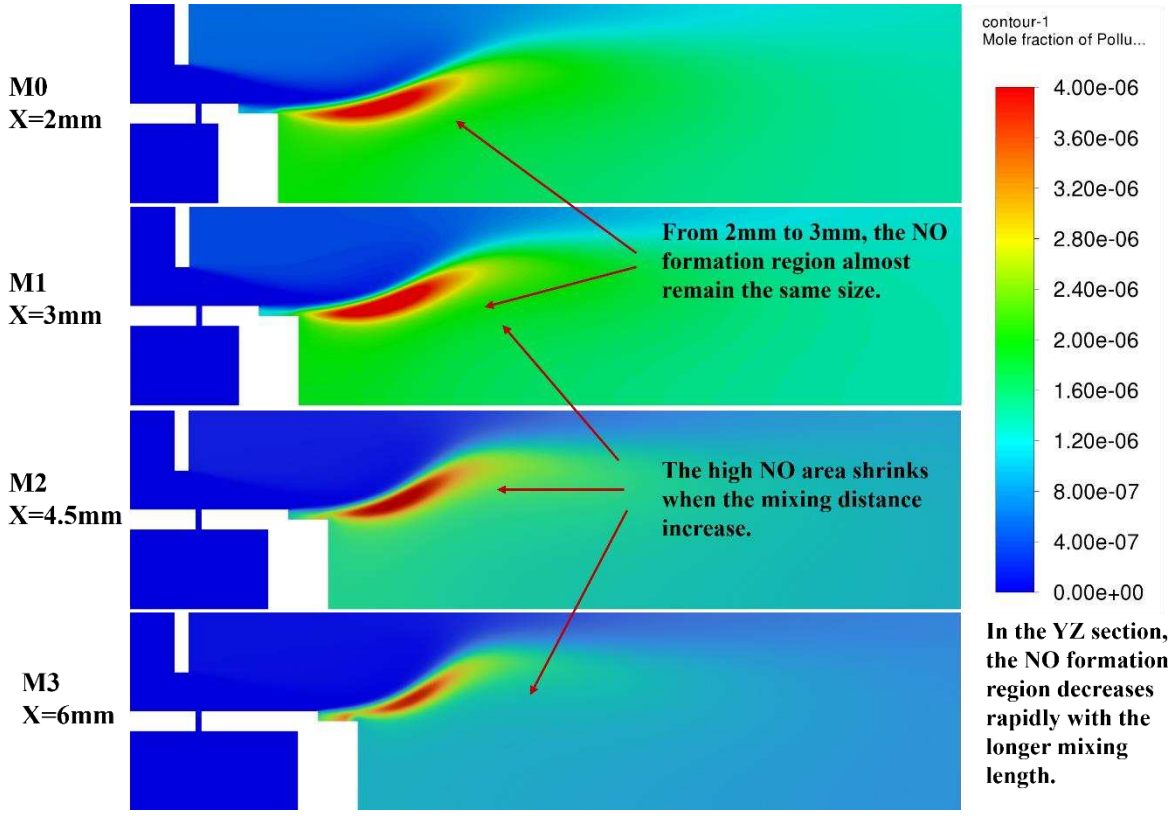

Figure 11. NO_X emission reduced with the mixing distance variation.

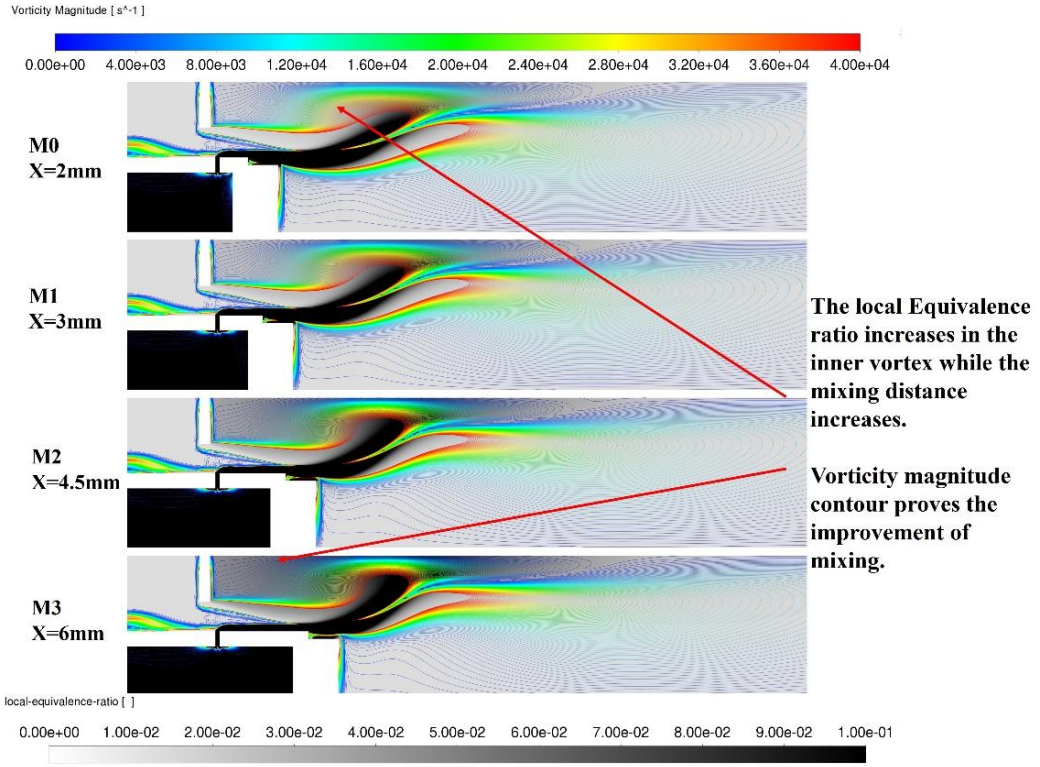

Figure 12. Local equivalence ratio and Vorticity magnitude contours with the mixing distance.

It can be deduced that extending the mixing distance effectively functions for reducing NO_X emissions. The increase in inner vortex size and vorticity magnitude improves the mixing ability of air and hydrogen. With the expansion of the recirculation area, more gases participate in turbulent movement, leading to more species being involved in the vortex and ensuring sufficient mixing of fuel and air. Additionally, in the optimised designs, the longer distance for hydrogen fuel to mix with oxidizers provides the fuel with a better opportunity to mix with more air, allowing the mixture to reach a lean burning condition before the ignition point.

To further verify this, the cases were simulated with different equivalence ratios ranging from 0.3 to 0.54 (0.3, 0.35, 0.4, 0.45, 0.5, 0.54). The numerical calculations were conducted using the FR/ED model, and the predicted NO_X emissions in parts per million (ppm) are listed in Table 2. This data has been plotted in Figure 13 to compare the differences in NO_X emissions between case M0 to case M3 under varying air/fuel ratio conditions.

It can be seen intuitively that when the mixing length is extended, the NO_X emissions are reduced, especially under high equivalence ratios where the inlet air is less, the effect on NO_X emissions

reduction is particularly obvious. Among all the modified cases, case M3 consistently exhibits the lowest emissions at each equivalence ratio point. Compared to the original design case M0, the reduction in NO_X emissions exceeds 5 ppm at an equivalence ratio of $\phi = 0.54$.

The modified cases show notable NO_X reduction at high equivalence ratios, suggesting enhanced performance with increased fuel fraction. This is attributed to the pivotal role of mixing intensity under rich fuel conditions. Elevated fuel/air ratios can lead to incomplete combustion, causing higher temperatures and increased NO_X emissions. Enhancing the mixing strength is essential in this context, as it promote efficient fuel-air mixing, thus reducing temperature and emissions.

Equivalence ratio	M0 x=2mm	M1 x=3mm	M2 x=4.5mm	M3 x=6mm
0.3	0.21	0.19	0.18	0.16
0.35	0.51	0.49	0.41	0.33
0.4	1.09	1.05	0.84	0.66
0.45	2.81	2.53	1.98	1.53
0.5	7.57	6.66	5.36	4.38
0.54	16.70	15.19	12.07	11.55

Table 2. The NO_X emission of variation mixing distance with different A/F ratios.

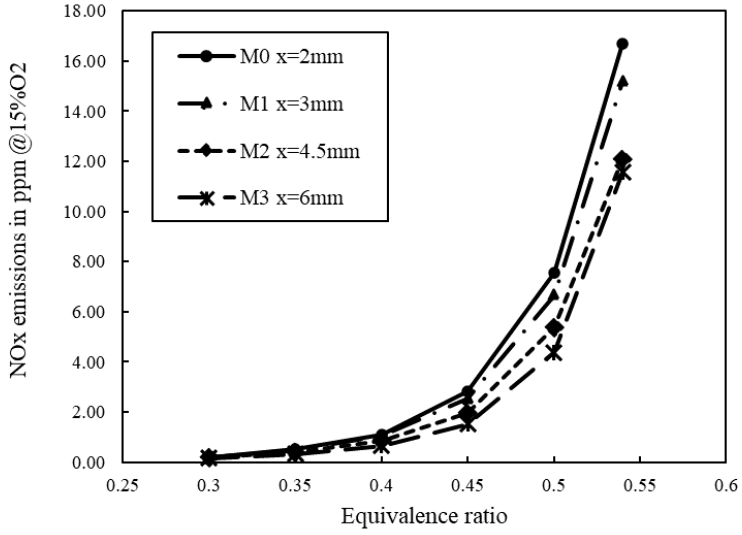

Figure 13. NO_X emission at different equivalence ratios of modified cases.

3.3 The effect of air gate height variation on NO_X emission

In previous studies by Funke et al.[60], [84] which primarily focused on the overall structural changes of air guiding panel, more attention was given to the combined effects of modifying both the air guiding panel and hydrogen segment dimensions. However, this paper will focus specifically on investigating the influence of air gate height variations its impact on NO_X emissions.

The overall dimension of the burner is kept the same, while the air speed variation with optimised air gate height is investigated to study the geometric parameters' effects on NO_X emissions.

The air gate height of the basic burner design is 1.95mm, to explore the effect of the height variation, six design cases were simulated and compared. These include five modified cases, with dimensions ranging from 1.5mm to 2.4mm. Detailed parameters were calculated based on equation (1). These values are listed in Table 3 below. It can be seen that as the air gate height increases, the momentum flux ratio also grows, resulting in deeper penetration of the hydrogen fuel.

Case	Air gate height	Air velocity (m/s)	Momentum flux ratio	Injection depth (mm)
H0	1.95mm	100.00	0.53	0.22
H1	1.50mm	130.00	0.32	0.17
H2	1.65mm	118.18	0.38	0.19
H3	1.80mm	108.33	0.46	0.20
H4	2.25mm	86.67	0.71	0.25
H5	2.40mm	81.25	0.81	0.27

Table 3. Air gate height design cases information.

At equivalence ratio 0.4 condition, the micromix combustion in case H0 to H5 were simulated, and the NO_X emission in ppm is plotted in Figure 14. The curves clearly illustrate the trend; as the air gate height increases the NO_X emission increase rapidly. Comparing case H0 and case H5, where the air gate height increased by 0.45 mm, the NO_X amount at the outlet was nearly three times higher in FR/ED

model results. The NOx emission with EDC model shows a similar tendency, the slight increase in the height of the air gate can lead to a notable increase in NO_X emissions.

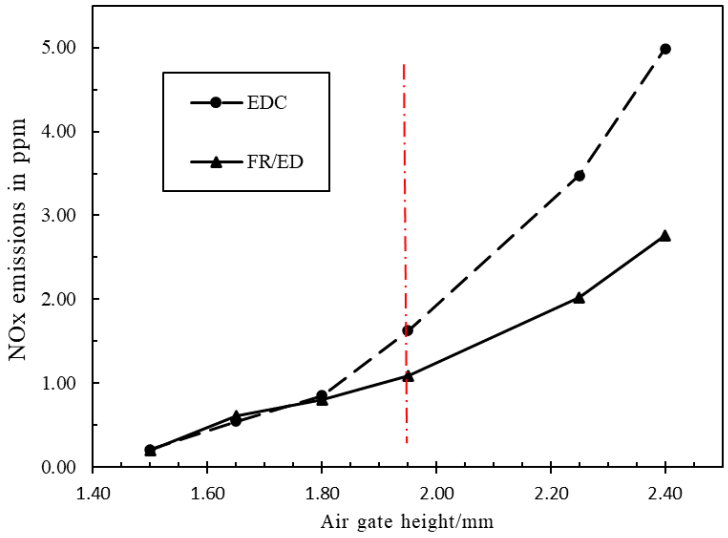

Figure 14. NO_X emission changes with the air gate height variation.

The temperature distribution contours for these six cases are shown in Figure 15 below, the contours reveal that as the height of the air gate increases, the burner's capability to reduce NO_X emissions declines. In the reduced air gate height group in Figure 15 (a) shows a good performance of temperature reduction, the area of the high-temperature zone is shrinking which corresponds to a significant reduction in nitrogen oxide emissions. Cases H1-H3 show a consistent and typical micromix flame shape, with the high-temperature zone distributed along the shear layer between the inner and outer vortices, maintaining relatively low chamber temperatures.

In contrast, in Figure 15 (b) the group with increased gate height demonstrates unexpected results. Compared to the baseline design H0, increasing the air gate height led to larger high-temperature zones, the length of the hot flame extending and thickening at gate heights exceeding 2mm. The heat of the flame has spread into the outer vortex, raising the downstream recirculated air temperature, which reduces the cooling efficiency of the outer vortex.

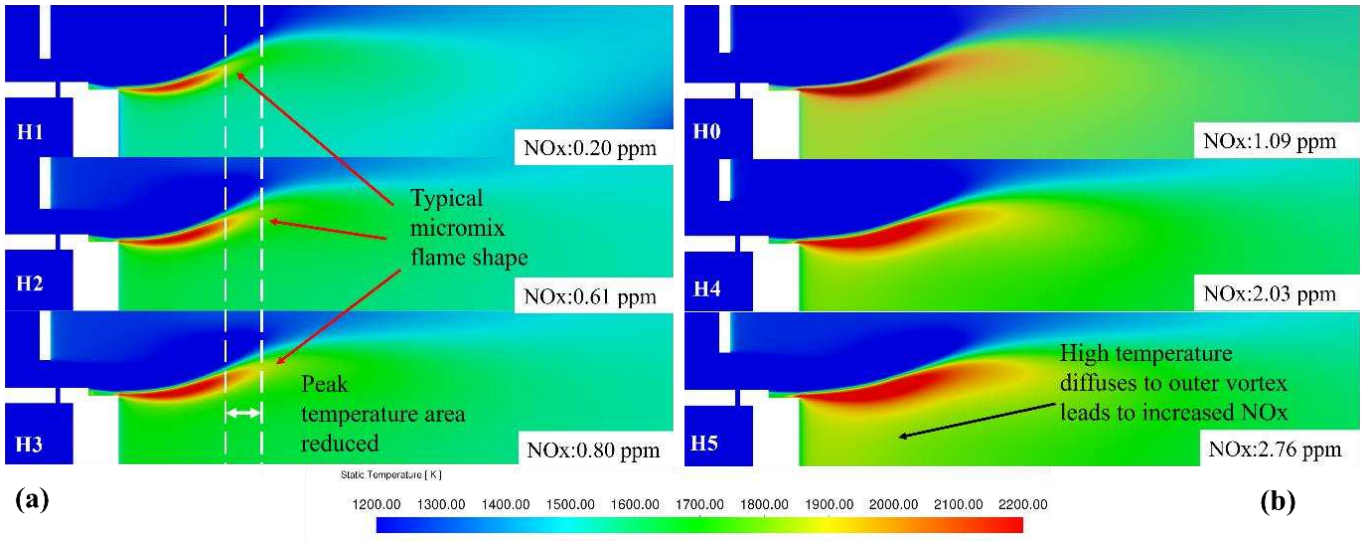

438

439 Figure 15. Temperature distribution contour of air gate height cases.

440 Case H5 performed the worst, with NO_X emissions more than ten times higher than in the best design
441 H1. Figure 16 (a) explains the reason of the high NO_X level in H5, from the colourmap it can be seen
442 that the pollutant distribution exactly matches the temperature contour, when high temperature
443 penetrates into the outer vortex, large amount of NO_X is formed, and its residence time increased due
444 to the larger high-temperature zone, leading to an exponential increase in NO_X emissions.

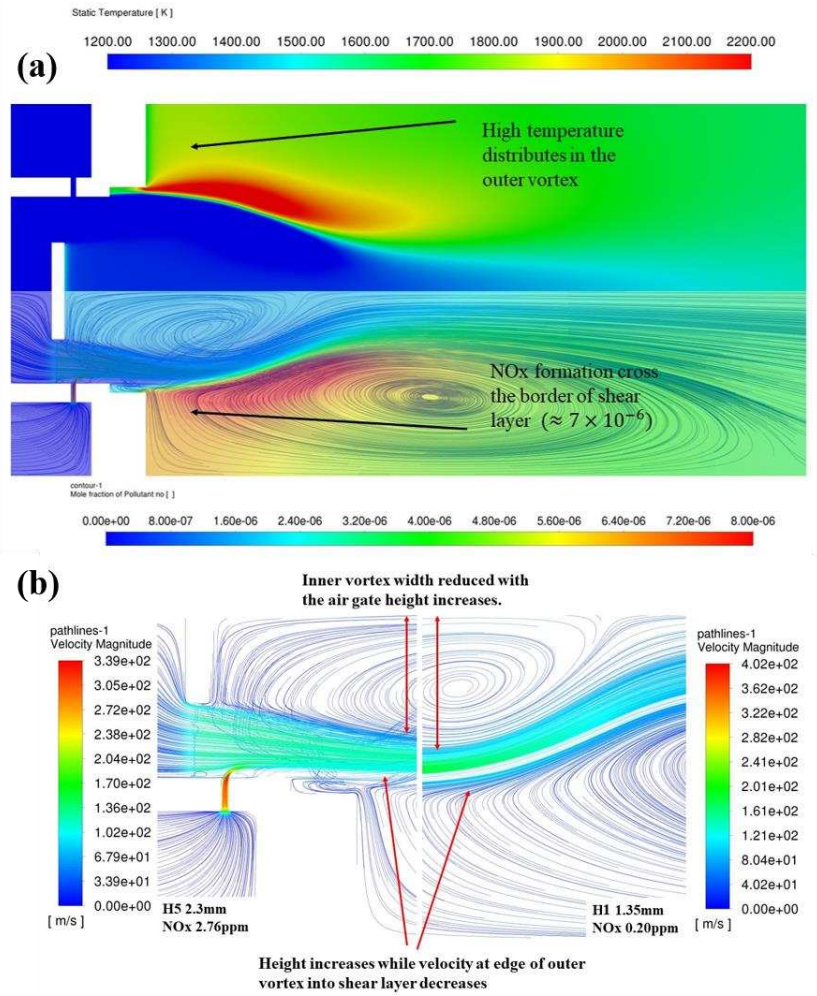

Figure 16. (a) NO_X and temperature distribution of H5. (b) The vortex size comparison between H1 and H5.

The flow structures of H1 and H5 are compared in Figure 16 (b), demonstrating that the larger air gate height results in a smaller inner vortex. In the H5 case, the width of the inner vortex decreases. As mentioned previously, changes in vortex size can affect mixing intensity, potentially contributing to increases in NO_X emissions. Speculation based on the above figures; another reason of higher NO_X production could be the velocity differences in these two cases. In case H5, the velocity at the edge of the outer vortex is lower than case H1, this makes the gas of vortex into the shear layer slower, the cooling efficiency of vortex reduced.

Further comparison of the mixing of fuel/air between cases H1 and H5 is illustrated in Figure 17 which shows the local equivalence ratio contours in the Gray-scale and vorticity magnitude in bgr-scale. From the figure, it could be found that with the lower air gate, in the inner vortex region, the contour colour of case H1 is lighter than case H5, which means that the local equivalence ratio is higher, and more fuel

458 has been involved in that region, the fuel and air exhibit better mixing in the inner vortex. The vorticity
459 value further proves this point, the vorticity value is higher in case H1, which means the lower air gate
460 could provide better mixing ability between fuel/air. The hollow area of vorticity contour reveals the
461 reason of lower gate has better NO_X reduction ability. As paper [85] indicates, vorticity is a key physical
462 characteries that measure the rotational intensity of a fluid, in H1, the high vorticity in the inner vortex
463 area indicates the intensive mixing in this area. The larger hollow area means more flow participates in
464 the mixing.

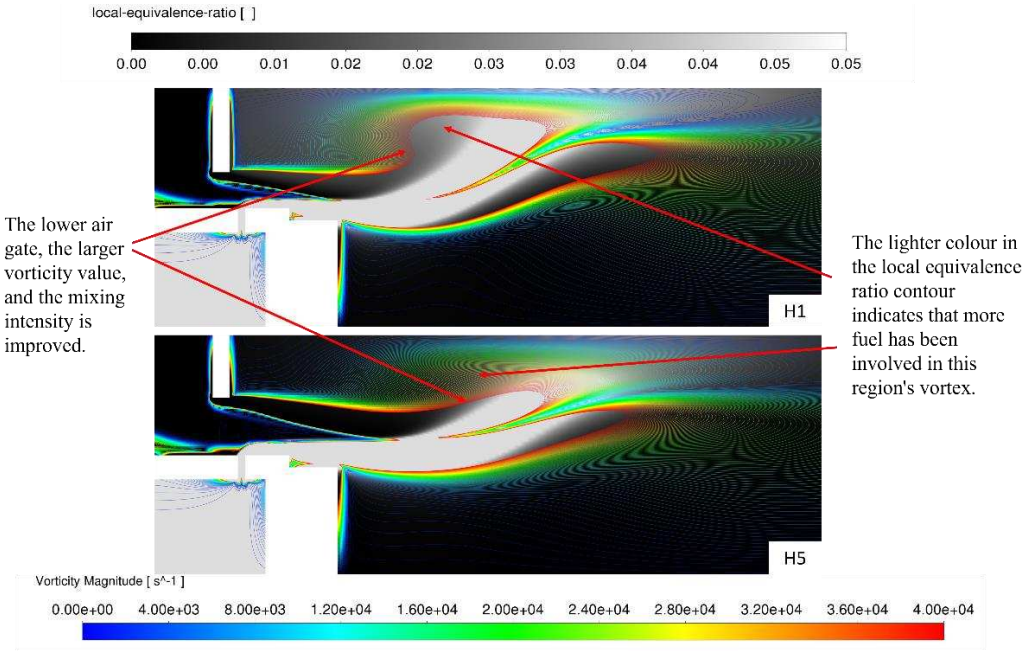

465

466 Figure 17. Local equivalence ratio and Vorticity magnitude contours of H1&H5.

467 Changes in flow dynamics within the micromix combustion chamber finally led to the variations in
468 combustion temperature which is a critical factor influencing NO_X formation. To better visualize the
469 temperature variation in the chamber, the X-Y facet maximum temperature along the chamber of case
470 H0, H1, H5 is plotted in Figure 18, the starting point of recording is the flame initiation position (4mm
471 from the air gate).
472 The curves clearly illustrate how the air gate design affects peak temperature in the combustor, the
473 temperatures distributed along the chamber are lower with the small air gate. In the peak temperature
474 region, approximately between 5.2mm to 11.5mm, the temperature at each position of design H5
475 (2.4mm) is, on average, 50K higher than that of the reference basic burner H0. Compared to the best

performance case H1 (1.5mm), the temperature drops significantly at each point, with an average difference of about 200K. Further downstream, the temperature between case H5 and H1 decreases significantly by about 400K. This confirms that reducing the air gate height can significantly lower micromix combustion temperature, which is essential for low- NO_X designs.

In addition to the decrease in peak temperature, the flame length also shortens from case H5 to case H1. At the position of Z=19 mm, the maximum temperature of case H1 has dropped to 1625 K, which is almost lower than the NO_X formation temperature. In contrast, the temperature in H5 remains above 1900 K, indicating sustained NO_X formation in this region.

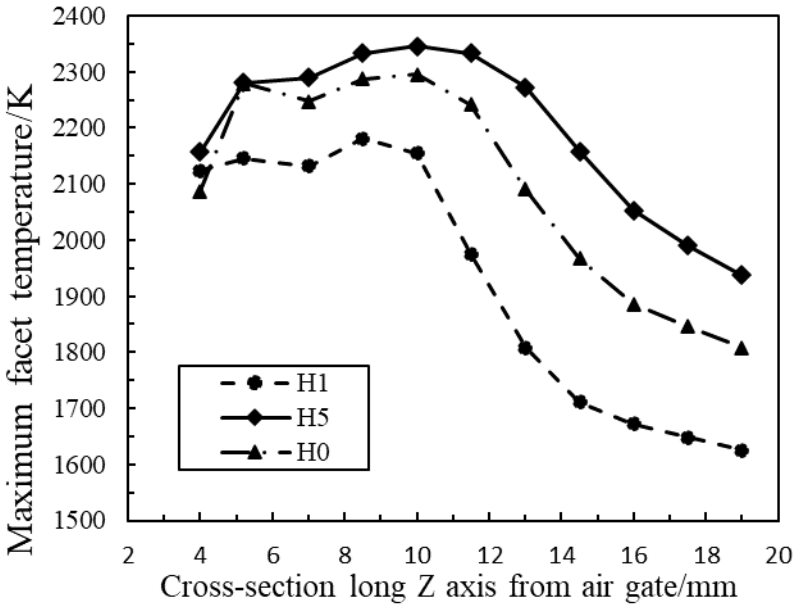

Figure 18. The comparison of maximum temperature along the chamber between cases H0, H1, and H5.

According to the theory of the jet-in-cross-flow from the papers [49], [86], [87], a longer injection penetration can improve mixing intensity and reduce NO_X emissions. The results above show an opposite trend, the biggest injection depth case H5 has the highest NO_X formation level. This does not necessarily indicate that the results of the simulation contradict the theory, as previous studies varied the upper section dimensions while keeping the air gate height constant to examine the effects of injection depth. In those cases, the thickness of the air stream would be the same as the gate height constant. The critical injection depth y_{crit} is determined by the air gate height, therefore, y_{crit} for each air gate height case in this study is variable. Comparing the injection depth and gate height, the penetration ratio would be a constant for these cases, the lower air gate would not cause the shallow

injection of hydrogen and lead to poor mixing. The lower air gate designs could increase the airspeed and improve the mixing of air and fuel, thereby finally achieving the research target.

4. Conclusion

This investigation focused on the geometric optimization of a micromix combustor with the aim of mitigating NO_X formation during hydrogen combustion. Several design scenarios were simulated using ANSYS Fluent, and the resultant numerical outcomes encompassing temperature profiles, flow dynamics, and NO_X formation were systematically compared and analysed. The results prove that reduction of NO_X emission could be achieved by physical modification to burner geometry.

- The mixing distance significantly affects flow structure and NO_X emission. In the comparison group, the mixing distance was increased from 2 mm to 6 mm. The results reflected that as the mixing distance increases, NO_X emissions gradually decrease. At higher equivalence ratio, the NO_X emission differences between varied mixing distances become more pronounced.
- The extension of the mixing distance has a limitation, the combustor component would be thicker and heavier due to the long distance which is not expected in practical usage. Thus, the mixing distance should be controlled in a suitable range.
- The air gate was designed with different heights to study the effect of air gate dimensions, the lower air gate has the best performance. The airflow accelerated due to the smaller air gate and resulted in the increasing mixing intensity; the structure of the vortex was also affected.
- The temperature along the chamber decreased with the lower air gate. For the smallest air gate, the temperature at the rear part of the burner was approximately 200 K lower than that of the basic burner. The NO_X emissions in case H1 were reduced by 80% compared to the basic burner.

Based on the points discussed above, the trends in the effects of geometry changes can be concluded. The longer mixing distance would undoubtedly aid in reducing NO_X emissions. The air gate height cases indicate that lower the air gates result in better combustion performance. The micromix burner could be further optimised by increasing the fuel penetration ratio. Increasing the inlet fuel pressure

is a feasible method to enhance the injection depth. Further studies are required to explore this aspect in more detail.

Acknowledgement

The authors would like to express their sincere gratitude to The University of Sheffield for providing support and resources throughout this research. Special thanks go to Dr. Bhupendra Khandelwal and Prof. Yang Zhang for their invaluable guidance, expertise, and encouragement throughout the course of this work.

Reference

[1] R. J. Andres *et al.*, "A synthesis of carbon dioxide emissions from fossil-fuel combustion," *Biogeosciences*, vol. 9, no. 5, pp. 1845–1871, 2012, doi: 10.5194/bg-9-1845-2012.

[2] Krein Axel and Williams Gareth, "Flightpath 2050: Europe's Vision for Aeronautics," in *Innovation for Sustainable Aviation in a Global Environment*, IOS Press, 2012. doi: 10.3233/978-1-61499-063-5-63.

[3] The Engineering toolbox, "Energy Storage Density." Accessed: Aug. 20, 2018. [Online]. Available: http://www.engineeringtoolbox.com/energy-density-d_1362.html.

[4] M. Sato and T. Hasegawa, "Reaction of fuel NOx formation for gas turbine conditions," *J Eng Gas Turbine Power*, vol. 120, no. 3, pp. 474–480, 1998, doi: 10.1115/1.2818169.

[5] F. Dahl, G., Suttrop, "Engine control and low-NOx combustion for hydrogen fuelled aircraft gas turbines," *Int J Hydrogen Energy*, vol. 23, no. 8, pp. 695–704, 1998, doi: 10.1016/S0360-3199(97)00115-8.

[6] F. Haglind and R. Singh, "Design of Aero Gas Turbines," *Engineering For Gas Turbine And Power*, vol. 128, no. 4, pp. 754–764, 2006, doi: 10.1115/1.2179468.

[7] Shelil N, "Flashback Studies with Premixed Swirl Combustion," Cardiff University, 2009.

[8] H. H.-W. Funke, S. Boerner, W. Krebs, and E. Wolf, "Experimental Characterization of Low NOx Micromix Prototype Combustors for Industrial Gas Turbine Applications," in *Volume 2: Combustion, Fuels and Emissions, Parts A and B*, ASMEDC, Jan. 2011, pp. 343–353. doi: 10.1115/GT2011-45305.

[9] H. H.-W. Funke, A. E. Robinson, and U. Ro¨nna, "Development and Testing of a 10 kW Diffusive Micromix Combustor for Hydrogen-Fuelled µ-Scale Gas Turbines," in *Volume 1: Aircraft Engine; Ceramics; Coal, Biomass and Alternative Fuels; Manufacturing, Materials and Metallurgy; Microturbines and Small Turbomachinery*, ASMEDC, Jan. 2008, pp. 651–658. doi: 10.1115/GT2008-50418.

[10] A. E. Robinson, H. H.-W. Funke, R. Wagemakers, J. Grossen, W. Bosschaerts, and P. Hendrick, "Numerical and Experimental Investigation of a Micromix Combustor for a Hydrogen Fuelled μ-Scale Gas Turbine," in *Volume 5: Microturbines and Small Turbomachinery; Oil and Gas Applications*, ASMEDC, Jan. 2009, pp. 253–261. doi: 10.1115/GT2009-60061.

[11] G. Dahl and F. Suttrop, "ENGINE CONTROL AND LOW-NO, COMBUSTION FOR HYDROGEN FUELLED AIRCRAFT GAS TURBINES," 1998.

[12] H. H-W Funke, N. Beckmann, J. Keinz, and A. Horikawa, "30 YEARS OF DRY LOW NOX MICROMIX COMBUSTOR RESEARCH FOR HYDROGEN-RICH FUELS: AN OVERVIEW OF PAST AND PRESENT ACTIVITIES," 2020. [Online]. Available: http://asmedigitalcollection.asme.org/GT/proceedings-pdf/GT2020/84133/V04BT04A069/6615525/v04bt04a069-gt2020-16328.pdf

[13] A. H. Ayed, K. Kusterer, H. H. W. Funke, J. Keinz, and D. Bohn, "CFD based exploration of the dry-low-NOx hydrogen micromix combustion technology at increased energy densities," *Propulsion and Power Research*, vol. 6, no. 1, pp. 15–24, Mar. 2017, doi: 10.1016/j.jppr.2017.01.005.

[14] H. H. W. Funke, N. Beckmann, and S. Abanteriba, "An overview on dry low NO x micromix combustor development for hydrogen-rich gas turbine applications," *Int J Hydrogen Energy*, vol. 44, no. 13, pp. 6978–6990, Mar. 2019, doi: 10.1016/j.ijhydene.2019.01.161.

[15] E. Recker, W. Bosschaerts, R. Wagemakers, P. Hendrick, H. Funke, and S. Börner, "Experimental study of a round jet in cross-flow at low momentum ratio," in *15th Int Symp on Applications of Laser Techniques to Fluid Mechanics*, Lisbon, Jul. 2010. Accessed: Apr. 25, 2025. [Online]. Available: https://www.semanticscholar.org/paper/Experimental-study-of-a-round-jet-in-cross-flow-at-Recker-Bosschaerts/7cca9a5f8ad5e6c5bdc31afd63118fdf52133515

[16] S. Boerner, -W Funke, P. Hendrick, E. Recker, R. Elsing, and R. M. Academy, "Development and integration of a scalable low NO x combustion chamber for a hydrogen fuelled aero gas turbine," 2011.

[17] A. Haj Ayed, K. Kusterer, H. H. W. Funke, J. Keinz, C. Striegan, and D. Bohn, “Experimental and numerical investigations of the dry-low-NOx hydrogen micromix combustion chamber of an industrial gas turbine,” *Propulsion and Power Research*, vol. 4, no. 3, pp. 123–131, Sep. 2015, doi: 10.1016/j.jppr.2015.07.005.

[18] A. Haj Ayed, K. Kusterer, H. H. W. Funke, J. Keinz, C. Striegan, and D. Bohn, “Improvement study for the dry-low-NOx hydrogen micromix combustion technology,” *Propulsion and Power Research*, vol. 4, no. 3, pp. 132–140, Sep. 2015, doi: 10.1016/j.jppr.2015.07.003.

[19] S. Boerner, -W Funke, P. Hendrick, E. Recker, R. Elsing, and R. M. Academy, “Development and integration of a scalable low NO x combustion chamber for a hydrogen fuelled aero gas turbine,” 2011.

[20] H. H.-W. Funke, J. Dickhoff, J. Keinz, A. H. Ayed, A. Parente, and P. Hendrick, “Experimental and Numerical Study of the Micromix Combustion Principle Applied for Hydrogen and Hydrogen-Rich Syngas as Fuel with Increased Energy Density for Industrial Gas Turbine Applications,” *Energy Procedia*, vol. 61, pp. 1736–1739, 2014, doi: 10.1016/j.egypro.2014.12.201.

[21] H. H. W. Funke, N. Beckmann, J. Keinz, and S. Abanteriba, “Comparison of Numerical Combustion Models for Hydrogen and Hydrogen-Rich Syngas Applied for Dry-Low-Nox-Micromix-Combustion,” *J Eng Gas Turbine Power*, vol. 140, no. 8, Aug. 2018, doi: 10.1115/1.4038882.

[22] H. Funke, N. Tekin, M. Ashikaga, and A. Horikawa, “Enhancement of fuel flexibility of industrial gas turbines by development of innovative hydrogen combustion systems Dry Low NOx Micromix Combustion with H2/CH4 Fuels View project Development of an innovative cooling technology for gas turbines View project Nurettin Tekin Enhancement of fuel flexibility of industrial gas turbines by development of innovative hydrogen combustion systems.” [Online]. Available: https://www.researchgate.net/publication/332290711

606 [23] -W Funke *et al.*, “NUMERICAL AND EXPERIMENTAL CHARACTERIZATION OF LOW
607 NOX MICROMIX COMBUSTION PRINCIPLE FOR INDUSTRIAL HYDROGEN GAS
608 TURBINE APPLICATIONS,” 2012. [Online]. Available:
609 http://asmedigitalcollection.asme.org/GT/proceedings-
610 pdf/GT2012/44687/1069/4221499/1069_1.pdf

611 [24] H. H.-W. Funke *et al.*, “Experimental and Numerical Study on Optimizing the DLN Micromix
612 Hydrogen Combustion Principle for Industrial Gas Turbine Applications,” in *Volume 4A:
613 Combustion, Fuels and Emissions*, American Society of Mechanical Engineers, Jun. 2015. doi:
614 10.1115/GT2015-42043.

615 [25] H. Funke, N. Tekin, M. Ashikaga, and A. Horikawa, “Enhancement of fuel flexibility of
616 industrial gas turbines by development of innovative hydrogen combustion systems Dry Low
617 NOx Micromix,” 2019. [Online]. Available:
618 https://www.researchgate.net/publication/332290711

619 [26] C. Striegan *et al.*, “Numerical Combustion and Heat Transfer Simulations and Validation for a
620 Hydrogen Fueled ‘Micromix’ Test Combustor in Industrial Gas Turbine Applications,” in
621 *Volume 4B: Combustion, Fuels and Emissions*, American Society of Mechanical Engineers, Jun.
622 2017. doi: 10.1115/GT2017-64719.

623 [27] A. Horikawa, K. Okada, M. Ashikaga, M. Yamaguchi, Y. Douura, and Y. Akebi, “Hydrogen
624 Utilization–Development of Hydrogen Fueled Power Generation Technologies,” *Kawasaki
625 Heavy Industries–Technical Review, Special Issue: Hydrogen Energy Supply Chain*, no. 182, pp.
626 41–46, 2021.

627 [28] H. H.-W. Funke *et al.*, “Numerical and Experimental Characterization of Low NOx Micromix
628 Combustion Principle for Industrial Hydrogen Gas Turbine Applications,” in *Volume 2:
629 Combustion, Fuels and Emissions, Parts A and B*, American Society of Mechanical Engineers,
630 Jun. 2012, pp. 1069–1079. doi: 10.1115/GT2012-69421.

[29] A. Haj Ayed *et al.*, "Numerical Study on Increased Energy Density for the DLN Micromix Hydrogen Combustion Principle," in *Volume 4A: Combustion, Fuels and Emissions*, American Society of Mechanical Engineers, Jun. 2014. doi: 10.1115/GT2014-25848.

[30] A. Giannouloudis *et al.*, "On the Development of an Experimental Rig for Hydrogen Micromix Combustion Testing," 2021. [Online]. Available: https://www.researchgate.net/publication/352844813

[31] G. Singh, B. D. J. Schreiner, X. Sun, and V. Sethi, "A review of hydrogen micromix combustion technologies for gas turbine applications," May 13, 2025, *Elsevier Ltd.* doi: 10.1016/j.ijhydene.2025.04.007.

[32] P. Agarwal, X. Sun, P. Q. Gauthier, and V. Sethi, "Injector Design Space Exploration for an Ultra-Low NOx Hydrogen Micromix Combustion System," in *Volume 3: Coal, Biomass, Hydrogen, and Alternative Fuels; Cycle Innovations; Electric Power; Industrial and Cogeneration; Organic Rankine Cycle Power Systems*, American Society of Mechanical Engineers, Jun. 2019. doi: 10.1115/GT2019-90833.

[33] M. López-Juárez, X. Sun, B. Sethi, P. Gauthier, and D. Abbott, "CHARACTERISING HYDROGEN MICROMIX FLAMES: COMBUSTION MODEL CALIBRATION AND EVALUATION," 2020. [Online]. Available: http://asmedigitalcollection.asme.org/GT/proceedings-pdf/GT2020/84119/V003T03A008/6614918/v003t03a008-gt2020-14893.pdf

[34] X. Sun *et al.*, "Numerical Investigation on the Geometrical Scaling of Hydrogen Micromix Injectors," in *Volume 2: Ceramics and Ceramic Composites; Coal, Biomass, Hydrogen, and Alternative Fuels*, American Society of Mechanical Engineers, Jun. 2024. doi: 10.1115/GT2024-128859.

[35] G. Lopez-Ruiz, I. Alava, and J. M. Blanco, "Impact of H2/CH4 blends on the flexibility of micromix burners applied to industrial combustion systems," *Energy*, vol. 270, May 2023, doi: 10.1016/j.energy.2023.126882.

[36] G. Lopez-Ruiz, I. Alava, and J. M. Blanco, “Study on the feasibility of the micromix combustion principle in low NO H2 burners for domestic and industrial boilers: A numerical approach,” *Energy*, vol. 236, p. 121456, Dec. 2021, doi: 10.1016/j.energy.2021.121456.

[37] P. Barreiro, I. Alava, J. M. Blanco, and G. Lopez-Ruiz, “An assessment of the operating conditions of the micromix combustion principle for low NOx industrial hydrogen burners: Numerical and experimental approach,” *Int J Hydrogen Energy*, vol. 66, pp. 208–222, May 2024, doi: 10.1016/j.ijhydene.2024.04.052.

[38] J. Berger, “Scaling of an Aviation Hydrogen Micromix Injector Design for Industrial GT Combustion Applications,” *Aerotecnica Missili & Spazio*, vol. 100, no. 3, pp. 239–251, Sep. 2021, doi: 10.1007/s42496-021-00091-5.

[39] D. Mo, Y. Lin, Y. Liu, and X. Han, “Investigation on the coupling mechanism of streamwise and jet vortices of hydrogen micromix combustion,” *Int J Hydrogen Energy*, vol. 96, pp. 68–84, Dec. 2024, doi: 10.1016/j.ijhydene.2024.11.163.

[40] D. Mo, Y.-Z. Lin, X. Han, F.-M. Wang, and Z.-D. Ma, “Design Optimization of Outlet Temperature Distribution of Design Optimization of Outlet Temperature Distribution of Hydrogen Micromixing Diffusion Combustor Based on Hydrogen Micromixing Diffusion Combustor Based on Micro-turbojet Engine Micro-turbojet Engine * *”, doi: 10.16492/j.fjjs.2024.05.0004.

[41] C. Devriese, W. De Paepe, and R. Bastiaans, “Impact of momentum ratio on JICF mechanism in micromix combustor for a hydrogen mGT,” *Int J Hydrogen Energy*, vol. 91, pp. 1045–1057, Nov. 2024, doi: 10.1016/j.ijhydene.2024.10.164.

[42] C. Devriese, S. Snijders, W. De Paepe, and R. Bastiaans, “The Design and Optimisation of a 100% Hydrogen Micro Gas Turbine Micromix Combustor: Preliminary Hydrogen Injection Depth Characterisation Using Cold Flow Steady RANS,” in *Volume 7: Industrial and Cogeneration; Manufacturing Materials and Metallurgy; Microturbines, Turbochargers, and*

682 *Small Turbomachines; Oil & Gas Applications*, American Society of Mechanical Engineers, Jun.
683 2022. doi: 10.1115/GT2022-80805.

684 [43] X. Chen, H. Wang, X. Wang, X. Liu, and Y. Zhu, "Fuel/air mixing characteristics of a Micromix
685 burner for hydrogen-rich gas turbine," *Energy*, vol. 282, Nov. 2023, doi:
686 10.1016/j.energy.2023.128786.

687 [44] X. Chen, H. Wang, C. Wang, X. Wang, N. Wang, and X. Liu, "Numerical investigation into fuel–
688 air mixing characteristics and cold flow field of single hydrogen-rich Micromix nozzle," *Fuel*,
689 vol. 332, Jan. 2023, doi: 10.1016/j.fuel.2022.126181.

690 [45] M. Chen *et al.*, "Experimental and numerical simulation study of the effect of mixing on the
691 characteristics of swirl/non-swirl micromix flames," *Energy*, vol. 307, Oct. 2024, doi:
692 10.1016/j.energy.2024.132570.

693 [46] X. Liu, W. Shao, C. Liu, X. Bi, Y. Liu, and Y. Xiao, "Numerical study of a high-hydrogen
694 micromix model burner using flamelet-generated manifold," *Int J Hydrogen Energy*, vol. 46, no.
695 39, pp. 20750–20764, Jun. 2021, doi: 10.1016/j.ijhydene.2021.03.157.

696 [47] X. Liu *et al.*, "Cold flow characteristics of a novel high-hydrogen Micromix model burner based
697 on multiple confluent turbulent round jets," *Int J Hydrogen Energy*, vol. 46, no. 7, pp. 5776–
698 5789, Jan. 2021, doi: 10.1016/j.ijhydene.2020.11.012.

699 [48] A. Durocher *et al.*, "Characterization of a 5-nozzle array using premix/micromix injection for
700 hydrogen," *Applications in Energy and Combustion Science*, vol. 18, Jun. 2024, doi:
701 10.1016/j.jaecs.2024.100260.

702 [49] A. H. Ayed, K. Kusterer, H. H. Funke, and J. Keinz, "Experimental and numerical investigations
703 of the dry-low-NO x hydrogen micromix combustion chamber of an industrial gas turbine,"
704 *Propulsion and Power Research*, vol. 4, no. 3, pp. 123–131, 2015, doi:
705 10.1016/j.jppr.2015.07.005.

[50] A. Haj Ayed, “Numerical Characterization and Development of the Dry Low NOx High Hydrogen Content Fuel Micromix Combustion for Gas Turbine Applications,” *PhD Thesis*, no. March 2017, pp. 1–14, 2017.

[51] H. H. W. Funke *et al.*, “Experimental and numerical study on optimizing the dry low NOx micromix hydrogen combustion principle for industrial gas turbine applications,” *J Therm Sci Eng Appl*, vol. 9, no. 2, pp. 1–10, 2017, doi: 10.1115/1.4034849.

[52] C. Devriese, W. De Paepe, and R. Bastiaans, “Impact of momentum ratio on JICF mechanism in micromix combustor for a hydrogen mGT,” *Int J Hydrogen Energy*, vol. 91, no. August, pp. 1045–1057, 2024, doi: 10.1016/j.ijhydene.2024.10.164.

[53] E. Recker and W. Bosschaerts, “Experimental study of a round jet in cross-flow at low momentum ratio,” *15th Int Symp on Applications of Laser Techniques to Fluid Mechanics*, vol. 1, no. x, pp. 5–8, 2010.

[54] A. Haj Ayed, “Numerical Characterization and Development of the Dry Low NOx High Hydrogen Content Fuel Micromix Combustion for Gas Turbine Applications,” *PhD Thesis*, no. March 2017, pp. 1–14, 2017.

[55] F. Galeazzo, G. Donnert, P. Habisreuther, N. Zarzalis, R. Valdes, and W. Krebs, “Measurement and Simulation of Turbulent Mixing in a Jet in Crossflow,” in *ASME Turbo Expo 2010*, 2021. doi: 10.1115/GT2010-22709.

[56] H. H.-W. Funke *et al.*, “Experimental and Numerical Study on Optimizing the DLN Micromix Hydrogen Combustion Principle for Industrial Gas Turbine Applications,” in *Volume 4A: Combustion, Fuels and Emissions*, American Society of Mechanical Engineers, Jun. 2015, pp. 1–12. doi: 10.1115/GT2015-42043.

[57] A. H. Ayed, K. Kusterer, H. H. Funke, and J. Keinz, “Improvement study for the dry-low-NO x hydrogen micromix combustion technology,” *Propulsion and Power Research*, vol. 4, no. 3, pp. 132–140, 2015, doi: 10.1016/j.jppr.2015.07.003.

[58] G. Lopez-Ruiz, I. Alava, and J. M. Blanco, “Study on the feasibility of the micromix combustion principle in low NOx H2 burners for domestic and industrial boilers: A numerical approach,” *Energy*, vol. 236, p. 121456, 2021, doi: 10.1016/j.energy.2021.121456.

[59] C. Devriese, S. Snijders, W. De Paepe, and R. Bastiaans, “The Design and Optimisation of a 100% Hydrogen Micro Gas Turbine Micromix Combustor: Preliminary Hydrogen Injection Depth Characterisation Using Cold Flow Steady RANS,” pp. 1–10, 2022, doi: 10.1115/gt2022-80805.

[60] H. H. W. Funke *et al.*, “Experimental and numerical study on optimizing the dry low NOx micromix hydrogen combustion principle for industrial gas turbine applications,” *J Therm Sci Eng Appl*, vol. 9, no. 2, pp. 1–10, 2017, doi: 10.1115/1.4034849.

[61] F. R. Menter, “Two-equation eddy-viscosity turbulence models for engineering applications,” *AIAA Journal*, vol. 32, no. 8, pp. 1598–1605, 1994, doi: 10.2514/3.12149.

[62] F. Menter, “Zonal Two Equation k-w Turbulence Models For Aerodynamic Flows,” in *23rd Fluid Dynamics, Plasmadynamics, and Lasers Conference*, Reston, Virigina: American Institute of Aeronautics and Astronautics, Jul. 1993. doi: 10.2514/6.1993-2906.

[63] H. Yu and J. Thé, “Validation and optimization of SST k-ω turbulence model for pollutant dispersion within a building array,” *Atmos Environ*, vol. 145, pp. 225–238, Nov. 2016, doi: 10.1016/j.atmosenv.2016.09.043.

[64] G. Lopez-Ruiz, I. Alava, and J. M. Blanco, “Study on the feasibility of the micromix combustion principle in low NOx H2 burners for domestic and industrial boilers: A numerical approach,” *Energy*, vol. 236, p. 121456, 2021, doi: 10.1016/j.energy.2021.121456.

[65] R. Ben Abdallah, V. Sethi, P. Q. Gauthier, A. Martin, and R. David, “A Detailed Analytical Study of Hydrogen Reaction in a Novel Micromix Combustion System,” pp. 1–11, 2018.

[66] T. D. Canonsburg, *ANSYS Fluent Theory Guide*, vol. 15317, no. November. 2013.

[67] Y. B. Zel'dovich, "The Oxidation of Nitrogen in Combustion Explosions," *Acta Physicochimica U.S.S.R.*, vol. 21, pp. 577–628, 1946.

[68] R. K. Hanson and S. Salimian, "Survey of Rate Constants in the N/H/O System," in *Combustion Chemistry*, New York, NY: Springer New York, 1984, pp. 361–421. doi: 10.1007/978-1-4684-0186-8_6.

[69] H. H.-W. Funke *et al.*, "Experimental and Numerical Characterization of the Dry Low NOx Micromix Hydrogen Combustion Principle at Increased Energy Density for Industrial Hydrogen Gas Turbine Applications," in *Volume 1A: Combustion, Fuels and Emissions*, American Society of Mechanical Engineers, Jun. 2013, pp. 1–10. doi: 10.1115/GT2013-94771.

[70] C. Striegan *et al.*, "Numerical Combustion and Heat Transfer Simulations and Validation for a Hydrogen Fueled 'Micromix' Test Combustor in Industrial Gas Turbine Applications," in *Volume 4B: Combustion, Fuels and Emissions*, American Society of Mechanical Engineers, Jun. 2017, pp. 1–10. doi: 10.1115/GT2017-64719.

[71] A. H. Ayed *et al.*, "Numerical study on increased energy density for the DLN Micromix hydrogen combustion principle," *Proceedings of the ASME Turbo Expo*, vol. 4A, no. x, pp. 1–12, 2014, doi: 10.1115/GT2014-25848.

[72] Z. Hong, D. F. Davidson, and R. K. Hanson, "An improved H2/O2 mechanism based on recent shock tube/laser absorption measurements," *Combust Flame*, vol. 158, no. 4, pp. 633–644, Apr. 2011, doi: 10.1016/j.combustflame.2010.10.002.

[73] T. Varga *et al.*, "Optimization of a hydrogen combustion mechanism using both direct and indirect measurements," *Proceedings of the Combustion Institute*, vol. 35, no. 1, pp. 589–596, 2015, doi: 10.1016/j.proci.2014.06.071.

[74] X. Li, X. You, F. Wu, and C. K. Law, "Uncertainty analysis of the kinetic model prediction for high-pressure H2/CO combustion," *Proceedings of the Combustion Institute*, vol. 35, no. 1, pp. 617–624, 2015, doi: 10.1016/j.proci.2014.07.047.

[75] H. J. Curran, J. M. Simmie, W. J. Pitz, O. Marcus, and C. K. Westbrook, "A Comprehensive Modeling Study of Hydrogen Oxidation," 2004, doi: 10.1002/kin.20036.

[76] I. G. Zsély, J. Zádor, and T. Turányi, "Uncertainty analysis of updated hydrogen and carbon monoxide oxidation mechanisms," *Proceedings of the Combustion Institute*, vol. 30, no. 1, pp. 1273–1281, 2005, doi: 10.1016/j.proci.2004.08.172.

[77] Z. Hong, D. F. Davidson, and R. K. Hanson, "An improved H2/O2 mechanism based on recent shock tube/laser absorption measurements," *Combust Flame*, vol. 158, no. 4, pp. 633–644, Apr. 2011, doi: 10.1016/j.combustflame.2010.10.002.

[78] M. P. Burke, M. Chaos, Y. Ju, F. L. Dryer, and S. J. Klippenstein, "Comprehensive H 2/O 2 kinetic model for high-pressure combustion," *Int J Chem Kinet*, vol. 44, no. 7, pp. 444–474, 2012, doi: 10.1002/kin.20603.

[79] A. Kéromnès *et al.*, "An experimental and detailed chemical kinetic modeling study of hydrogen and syngas mixture oxidation at elevated pressures," *Combust Flame*, vol. 160, no. 6, pp. 995–1011, 2013, doi: 10.1016/j.combustflame.2013.01.001.

[80] X. Li, X. You, F. Wu, and C. K. Law, "Uncertainty analysis of the kinetic model prediction for high-pressure H2/CO combustion," *Proceedings of the Combustion Institute*, vol. 35, no. 1, pp. 617–624, 2015, doi: 10.1016/j.proci.2014.07.047.

[81] T. Varga *et al.*, "Optimization of a hydrogen combustion mechanism using both direct and indirect measurements," *Proceedings of the Combustion Institute*, vol. 35, no. 1, pp. 589–596, 2015, doi: 10.1016/j.proci.2014.06.071.

[82] C. Olm, I. Gy, T. Varga, H. J. Curran, and T. Turányi, "Comparison of the performance of several recent syngas combustion mechanisms," *Combust Flame*, vol. 162, no. 5, pp. 1793–1812, 2015, doi: https://doi.org/10.1016/j.combustflame.2014.12.001.

[83] H. H. W. Funke, N. Beckmann, and S. Abanteriba, “An overview on dry low NO x micromix combustor development for hydrogen-rich gas turbine applications,” *Int J Hydrogen Energy*, vol. 44, no. 13, pp. 6978–6990, 2019, doi: 10.1016/j.ijhydene.2019.01.161.

[84] S. Boerner, H. H. Funke, P. Hendrick, and E. Recker, “Development And Integration of A Scalable Low NOx Combustion Chamber For A Hydrogen-fulled Aerogas Turbine,” *Progress in Propulsion Physics*, vol. 4, pp. 357–372, 2013, doi: 10.1051/eucass/201304.

[85] D. Mo, Y. Lin, Y. Liu, and X. Han, “International Journal of Hydrogen Energy Investigation on the coupling mechanism of streamwise and jet vortices of hydrogen micromix combustion,” vol. 96, no. November, pp. 68–84, 2024, doi: 10.1016/j.ijhydene.2024.11.163.

[86] J. Berger, “Scaling of an Aviation Hydrogen Micromix Injector Design for Industrial GT Combustion Applications,” *Aerotecnica Missili & Spazio*, vol. 100, no. 3, pp. 239–251, 2021, doi: 10.1007/s42496-021-00091-5.

[87] C. Devriese, S. Snijders, W. De Paepe, and R. Bastiaans, “The Design and Optimisation of a 100% Hydrogen Micro Gas Turbine Micromix Combustor: Preliminary Hydrogen Injection Depth Characterisation Using Cold Flow Steady RANS,” pp. 1–10, 2022, doi: 10.1115/gt2022-80805.